THERMAL WAVE CHARACTERIZATION OF SEMICONDUCTORS AND SUPERCONDUCTORS

Allan Rosencwaig, Jon Opsal, W.L. Smith and D.L. Willenborg

Therma-Wave, Inc.
47320 Mission Falls Ct.
Fremont, CA 94539

Thermal wave technology has proven to be a very effective means for investigating the near surface region of several different materials. Although there are many methods for generating and detecting thermal waves the most desirable for quantitative NDE are the noncontact and nondamaging laser methods. When a material is excited with an intensity-modulated laser pump beam a thermal wave is generated within the near surface of the sample. Since the complex refractive index of most materials depends on temperature, the laser pump induced modulations in the local temperature of the sample will induce a corresponding modulation in the local refractive index. This variation in refractive index can in turn be detected through the modulation in the reflectance of a laser probe beam from the surface of the material [1,2]. This method is not only a highly effective method for generating and detecting thermal waves, but also permits thermal wave measurements to be performed with micron scale spatial resolution by utilizing highly focused pump and probe laser beams.

Semiconductors

The laser pump generates thermal waves in all materials. In semiconductors, such as silicon, a pump laser operating in the visible also generates electron-hole plasma waves which also modulate the reflectance of the probe laser [2,3]. The thermal waves provide information about the local thermal transport properties while the plasma waves provide information about the local charge carrier transport properties. It is this latter sensitivity to local electrical properties that accounts for the success of the modulated reflectance method as a process control tool in the semiconductor industry for monitoring ion implant dose levels [4,5] and plasma-induced damage effects [6,7] in Si wafers.

In these applications no attempt is made to perform thermal wave imaging of individual defect structures in the silicon wafer. Recently we have demonstrated that the modulated reflectance method can be used to image localized defects and structures by employing high-density raster scanning techniques [8]. Images with 1 μm spatial resolution have been obtained of metallic precipitates, dislocations, dislocation clusters and stacking faults.

Figure 1 shows a line image of the thermal wave signal from a 40x20 μm region of silicon which has some Ni precipitates. The Ni precipitates strongly affect the plasma wave propagation through the local changes in both carrier mobility and lifetime and thus are readily seen by the modulated reflectance method. These precipitates cannot be detected by conventional optical imaging.

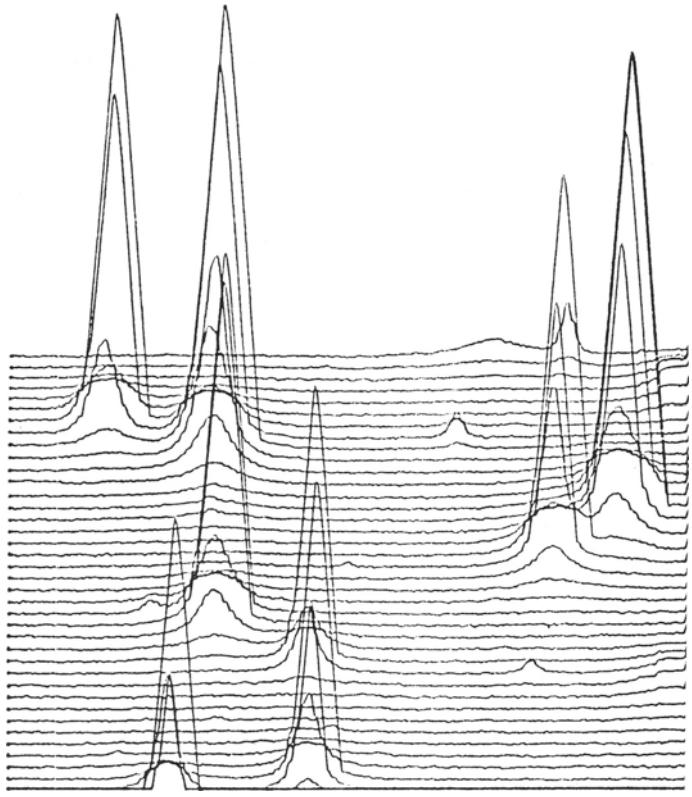

Fig.1 Modulated reflectance image of a 40x40 μm region of a Si wafer with Ni precipitates in the near surface region.

Metal precipitates are point defects that are very deleterious to IC device performance. The same is true of dislocations and stacking faults which are stable dislocation loops pinned at the surface. As with metal precipitates, dislocations and stacking faults are not optically visible and detection of these point defects is most often accomplished by wet chemical decorative etching. Although these etching procedures are simple and effective, they are destructive and thus have limited utility for in-line process control. The modulated reflectance method presents an effective nondestructive alternative.

This is illustrated in Fig. 2. Figure 2a shows a 50x50 μm modulated reflectance image of a Si wafer region containing two intersecting stacking faults located near a fiducial vertical line. In Fig. 2b we show the same region after decorative etch with the distinctive etched appearance of the stacking faults clearly visible. Note that in the thermal wave image the most prominent features are the three end pinning dislocations of these intersecting stacking faults.

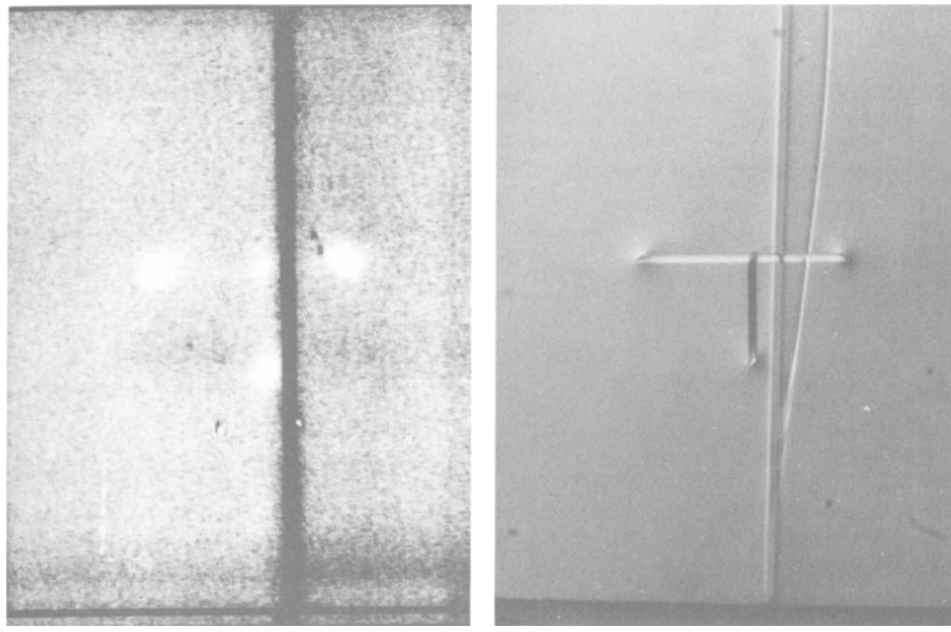

(a) (b)

Fig.2 (a) Modulated reflectance image (50x50 μm) of two intersecting stacking faults near a vertical fiducial line. (b) Optical image of the same two stacking faults after wet chemical decorative etch.

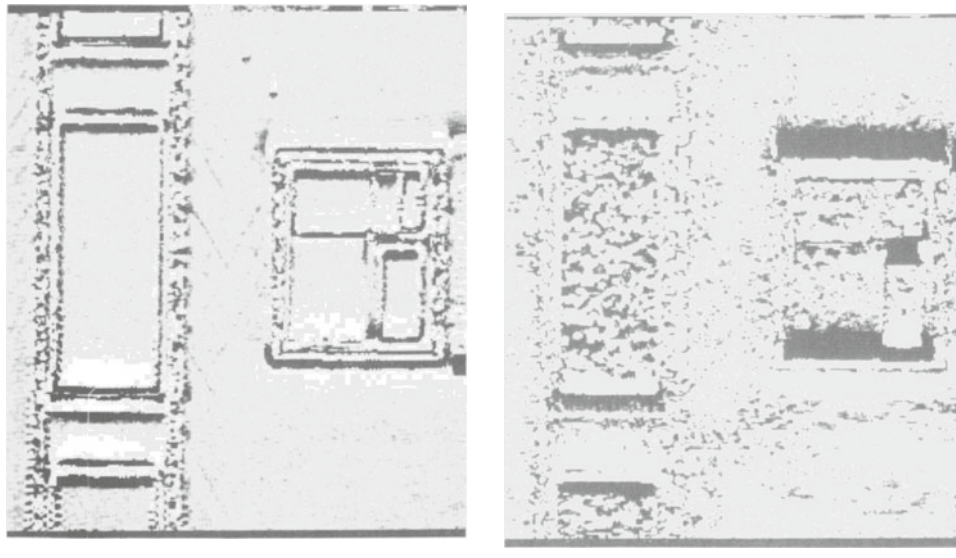

(a) (b)

Fig.3 (a) Optical image of a 100x100 μm region of an IC device. (b) Modulated reflectance image of same region showing presence of many poir defects.

Since the decorative etch process cannot be used on product wafers nondestructively it is of little value for process control. The modulated reflectance method can be used on product wafers in a totally nondestructive fashion and its utility for process control is illustrated in Fig. 3. Here we have imaged a 100x100 μm region of a malfunctioning IC device. Figure 3a shows the conventional optical image as obtained from the modulated reflectance system by recording the unmodulated HeNe probe reflectance. Figure 3b is the modulated reflectance image of the same region and shows the presence of a great many dislocations and stacking faults, clearly providing evidence that the degraded performance of this IC device was most likely due to the presence of these point defects.

The sensitivity of the modulated reflectance method to the presence of dislocations is illustrated in Fig. 4. Figure 4a is a 100x100 μm optical image of a virgin Si wafer that has been mechanically stressed to produce a dislocation density of $10^{12}/cm^3$. There is no evidence of these dislocations in the optical image. Figure 4b is the thermal wave image of the same region and clearly shows these dislocations preferentially ordered along the slip planes of the silicon crystal. The paper by J. Bailey, J. Opsal and E. Weber in this Proceedings gives further examples of modulated reflectance images of crystalline defects in silicon.

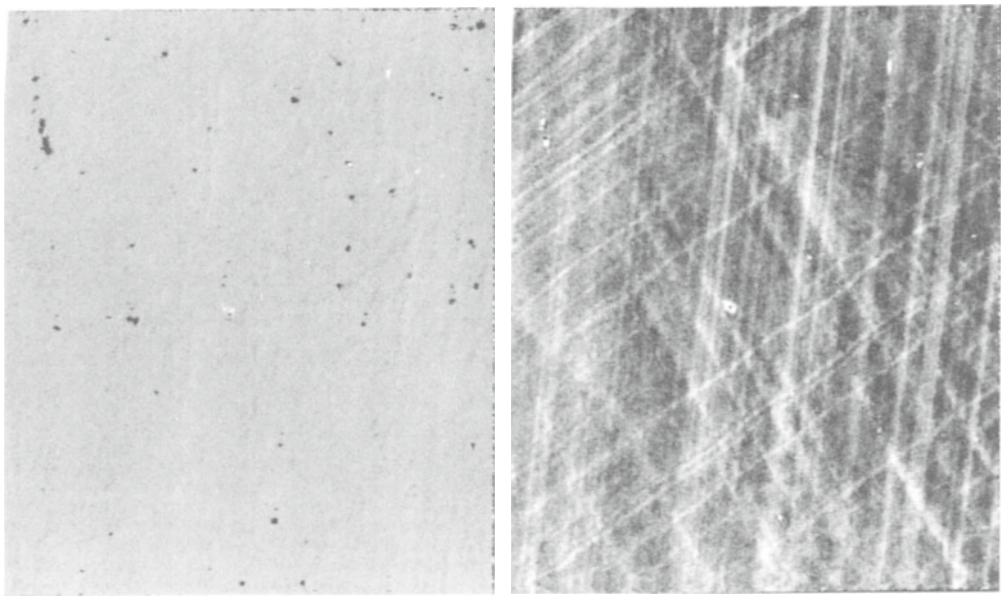

(a) (b)

Fig.4 (a) Optical image (100x100 μmm) of a mechanically stressed Si wafer. (b) Modulated reflectance image of same region showing dislocations preferentially ordered along crystallographic slip planes.

The various results described above indicate the potential of the modulated reflectance techniques for detecting and imaging a variety of point and crystallographic defects in silicon. The ability to obtain these images rapidly and nondestructively makes the technique highly useful for in-line process control in IC fabrication.

Superconductors

Since the discovery of high-T_c superconductors [9,10] there has been considerable activity focused on the syntheses and characterization of these new superconducting materials. Only a few of these characterization studies have concerned themselves with the thermal properties of these compounds [11-14]. Yet such studies could be of considerable value both for characterizing these new materials and for obtaining further insights into the physical origin of high-T_c superconductivity.

The studies to date on the thermal conductivity of the $YBa_2Cu_3O_{7-\delta}$ compound [11-13] indicate that the thermal conductivity undergoes a sizable increase as the temperature drops below T_c. This is attributed to the elimination of the electron-phonon scattering contribution to the thermal conductivity as the electrons condense into the superconducting state. Since thermal waves are directly influenced by the local thermal conductivity in a sample [15], a thermal wave image of a superconductor will be, in essence, an image of the local thermal conductivities in that material.

Figure 5 shows an optical (5a) and modulated reflectance (5b) image at room temperature of a 100x100 μm region of a sintered ceramic sample of superconducting $YBa_2Cu_3O_{7-\delta}$. Both images show considerable detail arising primarily from the heterogeneity in both optical and thermal properties of the various grains, pores and grain boundaries in this pressed ceramic.

Somewhat more intriguing images are shown in Figs. 6 and 7. These are room temperature optical and thermal wave images of a single crystal of superconducting $YBa_2Cu_3O_{7-\delta}$ obtained from H. Coufal of IBM Almaden Laboratory. The sample was a 200x200x20 μm single crystal with the growth face being the (a-b) plane and the 20 μm thickness along the c-axis. The

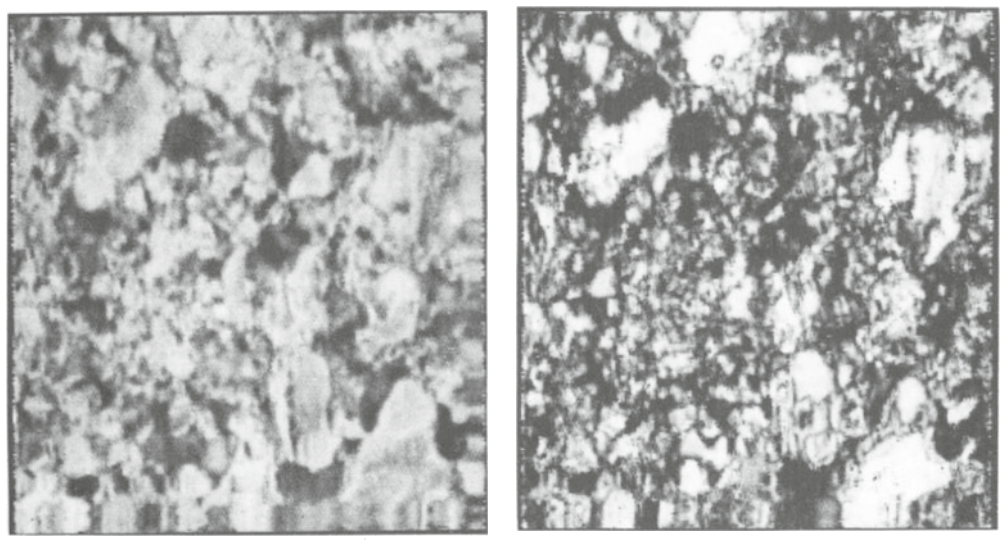

(a) (b)

Fig.5 Room temperature 100x100 μm optical image (a) and modulated reflectance image (b) of a sintered ceramic sample of superconducting $YBa_2Cu_3O_{7-\delta}$

optical images show the presence of a few defects and inclusions in both the (a-b) and (a-c) planes. The modulated reflectance images show the presence of many more crystallographic defects in both planes. In particular, the thermal wave image of the (a-b) plane indicates the presence of a major crystallographic boundary and cell-like structures that may be indicative of local variations in oxygen concentration.

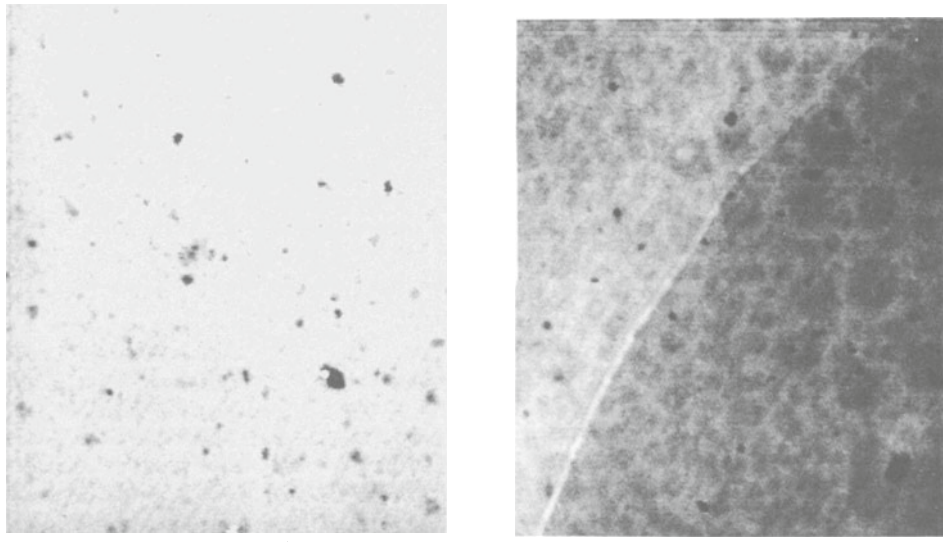

(a) (b)

Fig.6 Room temperature 100x100 μm optical (a) and modulated reflectance (b) images of the (a-b) plane in a single crystal of $YBa_2Cu_3O_{7-\delta}$

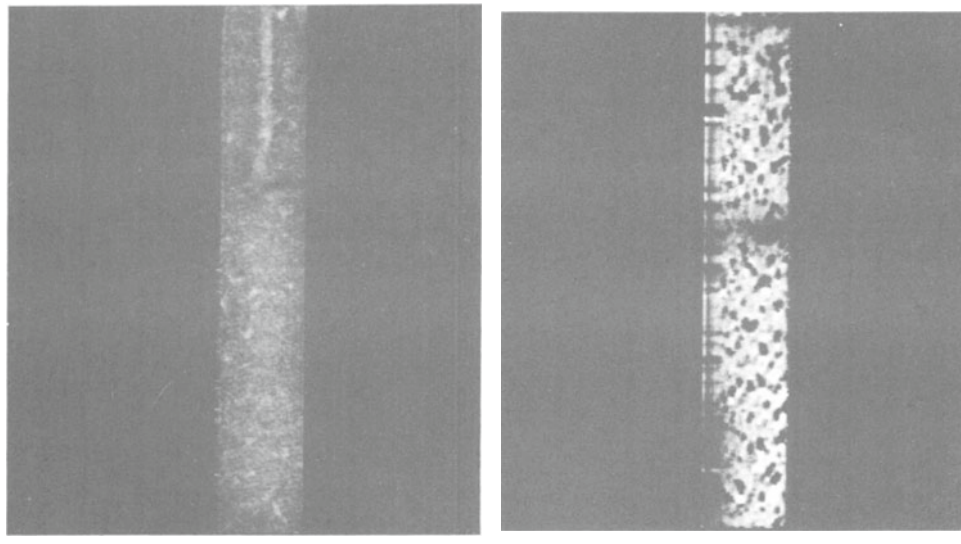

(a) (b)

Fig.7 Room temperature optical (a) and modulated reflectance (b) images of the (a-c) plane in a single crystal of superconducting $YBa_2Cu_3O_{7-\delta}$ The c-axis is along the 20 μm width.

Although these are very preliminary results they indicate the potential for thermal wave imaging of high-T_c superconducting materials. Of particular interest is the possibility that thermal wave imaging performed as a function of temperature could provide valuable information about the local microscopic superconductive properties in high-T_c materials. In such a study we would take advantage of the fact that the local thermal conductivity will undergo a noticeable increase (and hence result in a noticeable change in thermal wave signal) as the local region becomes superconducting.

Finally we wish to report on a thermal wave study of the anisotropy in the room temperature thermal conductivity of a single crystal of superconducting $YBa_2Cu_3O_{7-\delta}$. Although it is expected that the thermal conductivity, just as the electrical conductivity, will be anistropic in this highly anisotropic material, no such study has as yet been reported. We have used our modulated reflectance system with its 1 μm laser spot to measure the thermal conductivity along the three crystallographic axes. We found that $K_a \simeq K_b$ and that $K_a/K_c \simeq 30\text{-}50$. These findings are of considerable interest since they correlate so well with the recently measured anisotropies in the room temperature electrical conductivity [16], i.e., $\sigma_a \simeq \sigma_b$ and $\sigma_a/\sigma_c \simeq 30$. This correlation between the room temperature anisotropies in the thermal and electrical conductivities may simply be the result of the underlying crystallographic anisotropy. Or it may be indicative of a strong electron-phonon coupling as well. This might be determined by a study of the thermal anisotropy as a function of sample temperature. Since large crystals of high-T_c materials are difficult if not impossible to obtain such studies might best be performed with the high spatial resolution modulated reflectance method.

REFERENCES

1. A. Rosencwaig, J. Opsal, W.L. Smith and D.L. Willenborg, Appl. Phys. Lett. 46, 1013 (1985).
2. J. Opsal and A. Rosencwaig, in Review of Progressive in Quantitative NDE, edited by D.O. Thompson and D.E. Chimenti (Plenum Press, New York, 1988), Vol. 7A, pp. 215-224.
3. J. Opsal and A. Rosencwaig, Appl. Phys. Lett. 47, 498 (1985).
4. W.L. Smith, A. Rosencwaig and D.L. Willenborg, Appl. Phys. Lett. 47, 584 (1985).
5. W.L. Smith, A. Rosencwaig, D.L. Willenborg, J. Opsal and M.W. Taylor, Solid State Tech. 29, 85 January (1986).
6. P. Geraghty and W.L. Smith, Matl. Res. Soc. Proc. 68, 387 (1986).
7. R. Patrick, W.L. Smith and S. Salismian, Semicond. Intl. 9, 144 August (1988).
8. B. Witowski, W.L. Smith and D.L. Willenborg, Appl. Phys. Lett. 52, 640 (1988).
9. J.G. Bednorz and K.A. Müller, Z. Phys. B 64, 189 (1986).
10. C.W. Chu, P.H. Hor, R.L. Menz, L. Gao, Z.J. Huang and Y.Q. Wang, Phys. Rev. Lett. 58, 405 (1987).
11. C. Uher and A.B. Kaiser, Phys. Rev. B 36, 5680 (1987).
12. D.T. Morelli, J. Heremans and D.E. Swets, Phys. Rev. B 36, 3917 (1987).
13. J. Heremans, D.T. Morelli, G.W. Smith and S.C. Strite III, Phys. Rev. B 37, 1604 (1988).
14. L. Gomes, M.M.F. Vierra, S.L. Baldochi, N.B. Luma, M.A. Novak, N.D. Vieira Jr., S.P. Morato, A.J.P. Bragu, C.L. Cesar, A.F.S. Penna and J.M. Filko, J. Appl. Phys. 63, 5044 (1988).
15. A. Rosencwaig, Photoacoustics and Photoacoustic Spectroscopy, (John Wiley, New York, 1980).
16. S.W. Tozer, A.W. Kleinsasser, T. Penney, D. Kaiser and F. Holtzberg, Phys. Rev. Lett. 59, 1768 (1987).